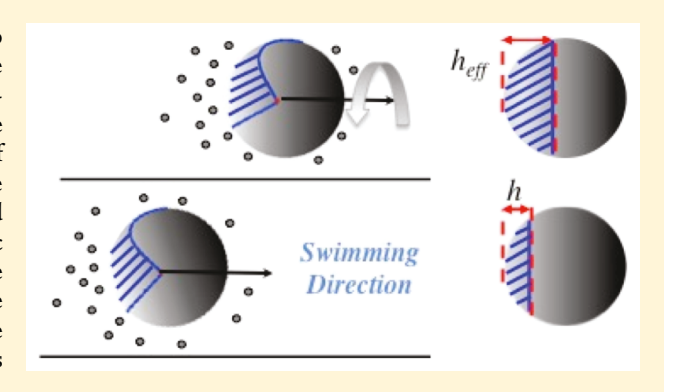
Experimental Study of the Motion of Patchy Particle Swimmers Near a Wall

Zohreh Jalilvand, Amar B. Pawar, and Ilona Kretzschmar*

Department of Chemical Engineering, City College of the City University of New York (CUNY), 140th Street & Convent Avenue, New York, New York 10031, United States

Supporting Information

ABSTRACT: In this work, we demonstrate our ability to precisely tailor the surface activity of self-propelled active colloids by varying the size of the active area. The quasi twodimensional autonomous motion of spherical patchy particle swimmers is studied in a chemical environment in the vicinity of a solid boundary. Oxidative decomposition of hydrogen peroxide into oxygen and water occurs only on a well-defined Pt-coated section of the polystyrene particle surface. The asymmetric distribution of product molecules interacting with the particle leads to the autonomous motion, which is characterized as the patch size varies from 11 to 25 to 50% of the particle surface area. The phoretic motion of patchy particle swimmers is analytically predicted by a model developed by Popescu et al.



and shows good agreement with the experimentally observed velocities when the influence of the wall on the preferential rotational motion of the particles near the solid boundary is considered. The study illustrates the potential to precisely engineer the motion of particles by controlling their properties rather than depending on changes in the environment.

INTRODUCTION

Downloaded by CITY COLG OF NEW YORK at 15:25:01:749 on June 30, 2019 from https://pubs.acs.org/doi/10.1021/acs.langmuir.8b03220.

Recently, nanoscale and microscale self-propelling swimmers have been a subject of growing interest among scientists. It has been demonstrated that synthetic self-propelling swimmers have the ability to move, carry, and transport components in fluidic environments. Thus, they have a wide variety of applications in medical diagnostics and the healthcare field, which include targeted drug delivery, 1-6 cancer fighting-agent delivery,⁷ and biopsy, cell sorting, and diagnostic assays.⁵ Further, cargo and lab-on-chip particle transport^{2,6,9-11} and environmental applications including contaminant removal and water quality monitoring have been reported. 12-14 To realize the potential applications mentioned above, understanding the generation and regulation of the autonomous motion is required. In this context, a much studied type of synthetic active colloids is the spherical Janus particle. The reactiondriven motion of Janus swimmers is caused by the asymmetric distribution of the surface reaction products around the particle. Although, recent literature shows that the swimming mechanism for microswimmers is still a matter of debate; the most commonly proposed mechanisms are bubble propulsion, ^{15–19} self-electrophoresis, ^{20–25} and self-diffusiophoresis. 26-30 The self-diffusiophoresis mechanism listed here refers to the self-phoretic motion induced by concentration gradients of the solute gradient around the swimmer. The driving force propelling the particle in a self-diffusiophoretic system arises from the intermolecular interaction between the solute

molecules and the colloid itself and is the mechanism used to describe the findings reported here.

In pursuit of a precise understanding of the motion of an active particle, more specifically a platinum (Pt)-coated particle, many experimental and theoretical studies have been carried out testing the impact of the particle size, fuel concentration, salt, cap thickness, and cap shape on the velocity and directionality of a swimmer's motion. For example, with regard to velocity regulation, Ebbens et al. studied, both experimentally and theoretically, the effect of the size of the swimmer on its swimming velocity. In their work, they showed that the swimming velocity is a complex function of particle size, that is, for radii from 250 nm to 2 μ m the swimming velocity decreases, whereas in the size range of 2-5 μ m, velocity is only a weak function of particle size.³¹ Furthermore, numerous studies have examined the influence of the fuel concentration (H₂O₂) on the swimming velocity. 28,31-33 The literature agrees that by increasing the fuel concentration, both the swimming velocity and the effective diffusion rate increase, which results in an enhanced motion of the active particles.

Investigating the effect of salt concentration on the active motion of Pt-capped Janus particles, 21,34,35 Ebbens et al. found that the swimming velocity and also the reaction rate both

Received: September 21, 2018 Revised: November 6, 2018 Published: November 7, 2018



seem to be functions of salt concentration as well as thickness variation within the cap. ²¹ To consolidate their findings, they suggest a combination of neutral and ionic diffusiophoresis and also electrophoretic effects. In contrast, Poon et al. have argued that all the observed ionic effects cannot be explained with a neutral or ionic diffusiophoresis mechanism because neither mechanism is able to provide sufficient ions to drive the observed swimming velocities. Hence, they conclude the mechanism for Pt-coated swimmers to be self-electrophoresis. ^{34,35}

Furthermore, concerning the directionality of the autonomous motion of swimmers, Ebbens et al. reported early on that the direction of motion of the swimmer particle is away from its catalytic cap, ³⁶ that is, the cap "pushes" the particle. Recently, numerous experimental and theoretical studies have probed the effect of the presence of a wall on the self-diffusiophoresis mechanism and the direction of the motion of the particles. ^{37–43} The theoretical studies show that the wall-induced distortion of both hydrodynamic and chemical fields around the particle contributes to the active motion of the particle yielding distinct behaviors, e.g., motion along the wall, steady hovering and/or reflection away from the wall.

Among all these studies, which have been designed to define the motion of the well-studied case of Janus particles, less attention has been devoted to the case of patchy particles where the particle is partially coated with the catalyst. Complimentary with these studies, a rational design of the motor itself by tailoring the catalytic patch size is another way to investigate the motion of synthetic swimmers. Although there are theoretical studies on the motion of patchy particle swimmers, there are only a few experimental reports on patchy particle swimmers and their motion. Patchy Ebbens et al. reported the controlled rotational motion of partially coated particles suspended in ${\rm H_2O_2}$ solution. A correlation between the glancing angle of deposition and the ratio of rotational to translational swimming velocity is proposed based on an electrokinetic mechanism.

In this context, motivated by the scarcity of experimental investigation of patchy particle swimmers, we aim to probe the motion and the phoretic behavior of patchy particles near a solid wall. In this study, to manipulate the swimmer's motion, the glancing angle deposition (GLAD) technique is used to break the symmetry of half-coated particles. 10,46 Our data shows that the autonomous motion of patchy particle swimmers can be controlled by the size of the catalytic patches. The phoretic velocity of the swimmers is measured as a function of patch size and it is observed that as the patch size increases from 11 to 25 to 50% of the particle surface, particle velocity increases and reaches a maximum at the patch size of 50%. In addition, we predict the patchy particle swimmer velocity using a model developed by Popescu et al.²⁹ Popescu's model is based on the framework of a standard theory of phoresis and describes the self-diffusiophoretic motion of patchy particle swimmers accurately. It verifies both the hypothesis of the swimming mechanism and also the preferential orientation of patchy particles with respect to the wall due to the hydrodynamic interaction between the swimmers and the wall. In this approach, the potential influence of the wall on the swimming behavior and also the alignment of the patchy particle swimmers with the wall are considered by introducing a new parameter—the effective height $(h_{\rm eff})$ of the patch—to fit the model to the experimentally observed patchy particle swimmer behavior.

EXPERIMENTAL DETAILS

The GLAD technique 10,46,47 is used to produce patchy particles with platinum (Pt) patches covering 50, 25, and 11% of the particle surface. Patchy particle swimmers are produced using sulfate latex (PS) particles with diameters of 2.4 and 5 $\mu \rm m$. In brief, plain PS particles are assembled into close-packed monolayers on a glass slide using a fast, convective assembly method and subsequently exposed to platinum vapor in a physical vapor deposition machine (Ted Pella). The angle of vapor deposition is precisely controlled using a mechanical stand to fabricate patchy particles with different surface coverages (90° for 50%, 30° for 25%, and 10° for 11%) of 10 nm thickness. 46

Figure 1A,B show scanning electron microscopy (SEM) images of 2.4 μ m PS latex particles with 25 and 11% Pt patches, respectively.

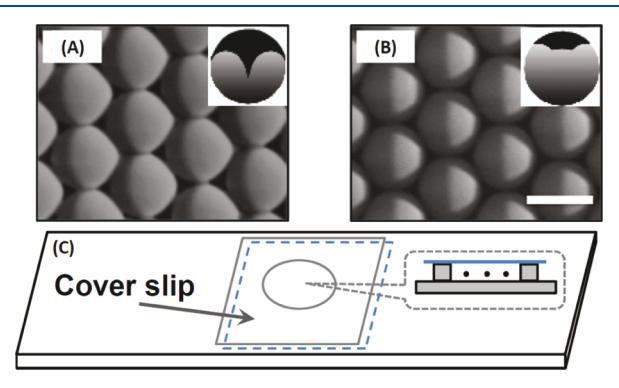


Figure 1. SEM images of 2.4 μm patchy particles with a monolayer orientation of $\alpha=0^{\circ}$ and vapor deposition angle of (A) $\theta=30^{\circ}$ and (B) $\theta=10^{\circ}$. Insets show the patch as predicted with the computational model.³⁹ (C) Sketch of the experimental cell with a cell height of 250 μm and cell volume of ~20 μL (inset: cross section of the cell).

The GLAD technique produces asymmetric patches on the particles as visualized by the insets in Figure 1A,B using mathematically modeled patch geometries. ⁴⁶ After deposition, patchy particles are dispersed in deionized water by sonication for 1 min. The dispersion of particles used in the experiments contains a mixture of patchy particles with various patch shapes albeit constant surface area generated because of different monolayer orientations with respect to the source. ⁴⁶ For experiments, the dispersion of patchy particles is mixed with an aqueous $\rm H_2O_2$ solution resulting in patchy particle swimmers, which are hereafter referred to as patchy swimmers.

The experimental cell used to study the patchy swimmer motion is composed of a precleaned glass slide and a microscope cover slide into which a spherical hole has been cut (Figure 1C). The cover slide with the hole is adhered to the precleaned glass slide with the help of a thin layer of Norland optical adhesive 63 (Norland Product, Inc). H_2O_2 solution [6% (v/v)] is prepared from an aqueous stock solution of 30% H₂O₂ (Fisher Scientific). During an experiment, the well is filled with 10 μ L of 6% (v/v) H₂O₂ solution. Then, an additional 10 µL of the patchy particle dispersion is added to the well and the mixture is gently mixed using a pipette tip resulting in a 3% (v/v) H₂O₂ solution in the well. The well is carefully covered with a second cover slip to avoid disturbance by air currents and to reduce evaporation. The autonomous motion of the patchy swimmers starts immediately after the two solutions are mixed in the well. In our studies, we measure the phoretic velocities within 5 min of mixing the two solutions. The volume fraction of patchy swimmers (<1%) is adjusted such that their motion is not affected by neighboring patchy swimmers. The patchy swimmer motion is observed using an Olympus BX-51 microscope with a ×20 objective. The trajectories of patchy swimmers are recorded for 60 s with a uEye 2240c camera at a rate of 10 frames per second. The motion of the patchy swimmers is analyzed using a modified MATLAB program originally written by Crocker, 48 which gives frame by frame the x,y coordinates of the

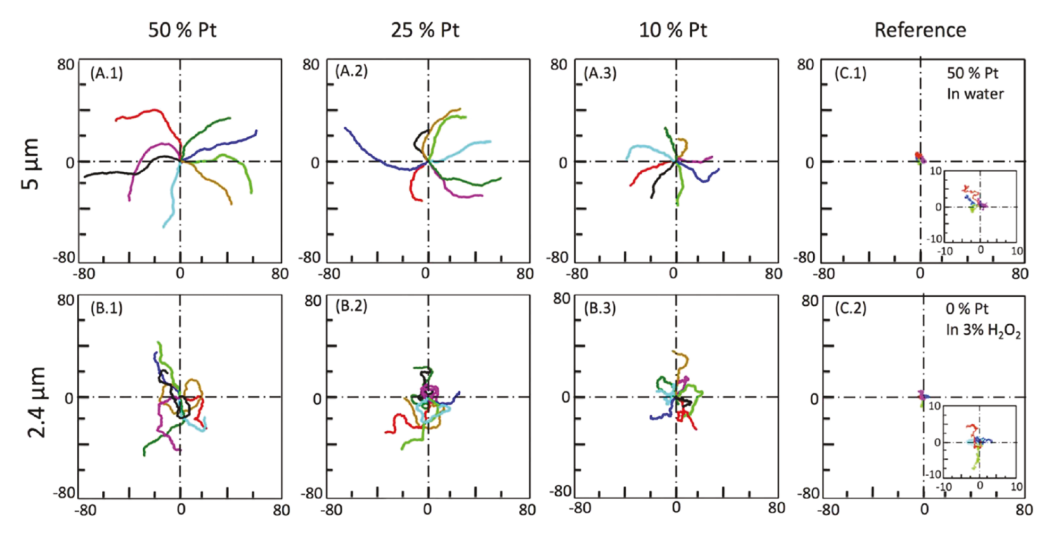


Figure 2. Representative 50 s trajectories of eight patchy swimmers in 3% (v/v) H_2O_2 solution. (A) 5 μ m PS particles with (A.1) 50, (A.2) 25, and (A.3) 11% platinum patches. (B) 2.4 μ m PS particles with (B.1) 50, (B.2) 25, and (B.3) 11% platinum patches. (C) Reference traces for four particles each under nonphoretic conditions: (C.1) 5 μ m particles with 50% patch in water and (C.2) 2.4 μ m particles without patches in 3% (v/v) H_2O_2 . Insets show magnified version of plot.

patchy swimmers as a function of time. The trajectories are then analyzed using the procedure described in ref 24 to obtain phoretic velocities (V), diffusion coefficients (D), effective diffusion coefficients $(D_{\rm eff})$, and the rotational diffusion time $(\tau_{\rm R})$ from MSD plots (see Supporting Information, Figure S1A and Table S1).

RESULTS AND DISCUSSION

The motion of patchy swimmers is characterized by applying an established MSD analysis to their trajectories that provides a phoretic velocity and diffusion coefficient for each patchy swimmer. Figure 2 provides representative 50 s trajectories of 2.4 and 5 μ m patchy swimmers as the patch size is varied from (1) 50% to (2) 25% to (3) 11% of the particle surface. Comparison of the length of the trajectories in Figure 2 shows that increasing the angle of deposition induces an enhanced motion of the patchy swimmers because of the increasing patch size. Janus and patchy particles comprise active and passive components and their motion represents the competition between the active swimming and the passive Brownian motion. The direction of the motion is correlated to patchy swimmer's orientation, which is subjected to rotational diffusion with a characteristic time scale (τ_R) . At short times (where $\Delta t \ll \tau_{\rm R}$), the displacement (ΔL) of a particle being propelled is linear in time ($\Delta L \propto V \Delta t$), whereas, the contribution to the displacement due to random Brownian motion is proportional to the square root of time ($\Delta L \propto$ $(4D\Delta t)^{1/2}$). At longer times (where $\Delta t \gg \tau_{\rm R}$), patchy swimmers show a diffusive behavior with an effective diffusivity $D_{\text{eff}} = D + 0.25 V^2 \tau_{\text{R}}$, which represents a directional active motion coupled with Brownian rotational diffusion.^{28,49}

The 2D MSD versus time plots obtained are fitted using eqs 1 and 2 (Figure S1A) to determine parameters (Table 1, Figure S1B) such as phoretic velocity (V), diffusion coefficient (D), and rotational diffusion coefficient (τ_R) of the swimmer, as reported by Golestanian et al.²⁸ for Janus swimmers (see below).

$$\Delta L^2 = 4D\Delta t + V^2 \Delta t^2 \qquad \Delta t \ll \tau_{\rm R} \tag{1}$$

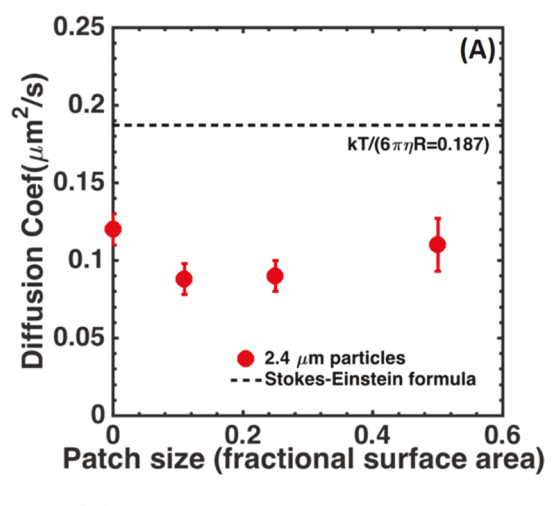
$$\Delta L^2 = (4D + V^2 \tau_R) \Delta t \qquad \Delta t \gg \tau_R \tag{2}$$

Table 1. Experimental Phoretic Velocities with One Standard Deviation Obtained from Fitting of MSD Data as a Function of Patch Size for 2.4 and 5 μ m Pt-Coated PS Particles Capped with 11, 25, and 50% Platinum Patches (See Text)

	11% area coated	25% area coated	50% area coated
2.4 μm	0.8 ± 0.1	1.4 ± 0.2	1.5 ± 0.2
$5 \mu m$	1.1 ± 0.1	1.3 ± 0.2	1.4 ± 0.2

Following the phoretic velocity analysis, diffusion coefficients for the patchy swimmers are extracted from the MSD measurements (Figure 3 and Table S1 in the Supporting Information). In theory, the diffusion coefficient of a spherical particle with radius R in the bulk, that is, 3D, is given by the Stokes-Einstein formula ($D = k_B T / 6\pi \mu R$, where k_B is the Boltzmann constant, T is the temperature, and μ is the viscosity of the medium), which amounts to 0.187 and 0.087 μ m²/s for 2.4 and 5 μ m particles, respectively (dashed lines in Figure 3A,B). The experimental measurements clearly deviate from the Stokes-Einstein prediction because of the presence of the solid wall. Figure 3 depicts the diffusion coefficients of active patchy particles, that is, patchy swimmers, and plain particles (patch size = 0) in comparison with the colloid in bulk water (dashed lines). Note that the system is quasi 2D, in which gravity and wall interactions hinder the motion of the particles away from the wall; however, the motion in the third dimension is still feasible, whereas in a 2D interface that would not be the case. The diffusion coefficient of the 5 μ m particles is 50% smaller than that of the 2.4 μ m particles owing to their bigger size and in agreement with the trend predicted by the Stokes-Einstein formula. Additional analysis of the trajectories of patchy swimmers in aqueous solution (see Figure S2, no fuel) shows that the experimental diffusion coefficients do not depend on the particle activity. Thus, the reduced diffusion coefficients observed are attributed to the hydrodynamic interaction of the swimmers with the wall. The asymmetric distribution of the solute around the swimmers, which is modified in the presence of the wall, may also contribute. 40,50

Table 1 Figure S1B in the Supporting Information show the experimental phoretic velocities of the patchy swimmers as a



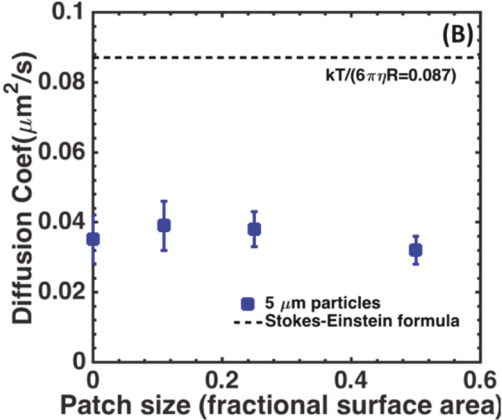


Figure 3. Experimental diffusion coefficients with error bars (one standard deviation) as a function of patch size for (A) 2.4 μ m (red circles) and (B) 5 μ m (blue squares) plain and Pt-coated PS particles capped with 11, 25, and 50% platinum patches. Black dashed lines represent 3D diffusion coefficients calculated using the Stokes–Einstein formula for 2.4 and 5 μ m particles, respectively (see text).

function of their patch size for 2.4 and 5 μ m particles. The experimental phoretic velocities are average velocities obtained from the analysis of 80 patchy swimmer trajectories (per data point) and the error range reported indicates one standard deviation. From the velocity data listed in Table 1, it is apparent that for both 2.4 and 5 μ m PS particles, the phoretic velocity increases with increasing patch size. Additionally, it can be noted that as the patch size becomes larger, the effect of the patch size on the phoretic velocity is diminished. Both particle sizes exhibit maximum velocity at a patch size of 50% (Janus case).

Different hypotheses have been suggested to describe the motion of Janus swimmers as mentioned earlier. $^{23-25,51-53}$ In our system, H_2O_2 is catalytically transformed into H_2O and O_2 on the Pt cap. Because oxygen bubbles are not observed on the Pt caps, the interfacial tension gradient is neglected and the motion of the patchy swimmers is described based on the concentration gradient of O_2 molecules around the particle. The driving force for particle motion then arises from the intermolecular interactions between the particle and solute molecules (O_2) , which are asymmetrically distributed around the particle, known as the self-diffusiophoresis mechanism.

A comparable kind of particle motion caused by a linear concentration gradient of solute molecules was originally

described by Anderson. S4 Golastanian et al. expanded Anderson's analysis to a diffusiophoretic motion of a spherical particle, and Popescu et al. generalized the approach for spheroidal particles that generate a solute gradient through a chemical reaction. In their study, the self-generation of the solute gradient is assigned to the catalytic conversion of solvent molecules (A) to products (A′ and B), which matches our catalytic conversion of H_2O_2 (A) into H_2O (A′) and O_2 (B). Popescu et al. analytically derived an expression for the phoretic velocity of a spherical patchy particle that is shown in eq 3

$$V_{\rm sph} = \frac{(1 - S_{\rm h})^2 - 1}{4} V_0 \tag{3}$$

where $S_h = h/R$, h is the height of the cap and R is the particle radius. V_0 is the velocity scale defined by eq 4

$$V_0 = \frac{b\nu_{\rm B}\sigma}{D} \text{ with } b = \frac{k_{\rm B}T\Lambda}{\mu}$$
 (4)

where b is the effective mobility coefficient, $\nu_{\rm B}$ is the reaction rate at the catalytic site, i.e., the number of product molecules created per unit time, σ is the number density, i.e., the number of catalytically active sites per unit area, D is the diffusion coefficient of the solute molecules, $D = k_{\rm B}T/6\pi\mu a$, $k_{\rm B}$ is the Boltzmann constant, T is the temperature, $\lambda = |\Lambda|^{0.5}$ is the characteristic interaction length scale, i.e., the interaction between the solute and particle and $\lambda = 5$ Å, μ is the viscosity (solute plus solvent), and a is the radius of the solute or product molecule. Further, for the catalytic decomposition of H_2O_2 , it follows that $\nu_{\rm B}\sigma = 2k$, where k is the overall reaction constant for the decomposition reaction (eq 5), which leads to a Michaelis—Menten type of kinetics (eq 6).

$$H_2O_2 + Pt \xrightarrow{k_1} Pt(H_2O_2) \xrightarrow{k_2} H_2O + O_2$$
 (5)

$$k = k_2 \frac{[H_2 O_2]_{\text{vol}}}{[H_2 O_2]_{\text{vol}} + k_2 / k_1}$$
(6)

The experimental velocities (Table 1) and analytically calculated phoretic velocities for the patchy swimmers are compared in Figure 4. The dashed line represents phoretic velocities calculated using eqs 3, 4, and 6 with the parameters a=0.6 Å, $\lambda=5$ Å, $k_1=4.4\times10^{11}~\mu\text{m}^{-2}~\text{s}^{-1}$, $k_2=4.8\times10^{10}~\mu\text{m}^{-2}~\text{s}^{-1}$, $\mu=1\times10^{-3}~\text{Pa}\cdot\text{s}$ at the condition of T=25~°C, and $[\text{H}_2\text{O}_2]_{\text{vol}}=3\%.^{28}$ In these calculations, the effect of patch size is taken into account by defining a fractional surface area, $S_h=h/R$, based on the assumption that the asymmetric patches are represented by hemispherical caps with the same area A symmetrically located at the pole of the particles, i.e., $S_h=h/R=2\times(\text{fractional surface area of the patch})$ as shown in Figure 5. Thus, $S_h=1$ represents a Janus swimmer, whereas $S_h=0.5$ and 0.22 for 25- and 11%-coated patchy swimmers, respectively.

Inspection of Figure 4 shows that despite the similar trend the analytically calculated phoretic velocities (dashed line) drastically underestimate the experimentally measured velocities for patchy swimmers with 11 and 25% patch sizes but agree well within the experimental error for the case of a 50%-coated (Janus) swimmer. More specifically, the predicted phoretic velocity is much lower than the experimentally observed velocity. The 50%-coated particle has, per definition, a hemispherical cap, explaining the excellent agreement in experimentally observed and analytically calculated phoretic

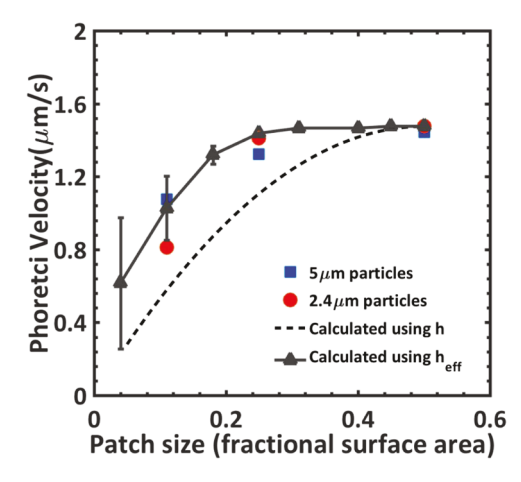


Figure 4. Comparison of experimental velocities (Table 1) obtained for 2.4 (red circles) and 5 μ m (blue squares) patchy swimmers to calculated phoretic velocities as a function of patch size. Dashed line: Phoretic velocities calculated by eq 3 and h assuming a symmetric patch (see text and Figure 5). Black triangles and solid line: calculated phoretic velocities using eq 3 and apparent $h_{\rm eff}$ values (see text and Figure 5) for pseudo-hemispherical patches. Error bars are the result of patch shape variation due to the monolayer orientation, α . Note: Error bars for experimental velocities (red circles and blue squares) are left out for clarity but are provided in Table 1 and Figure S1.

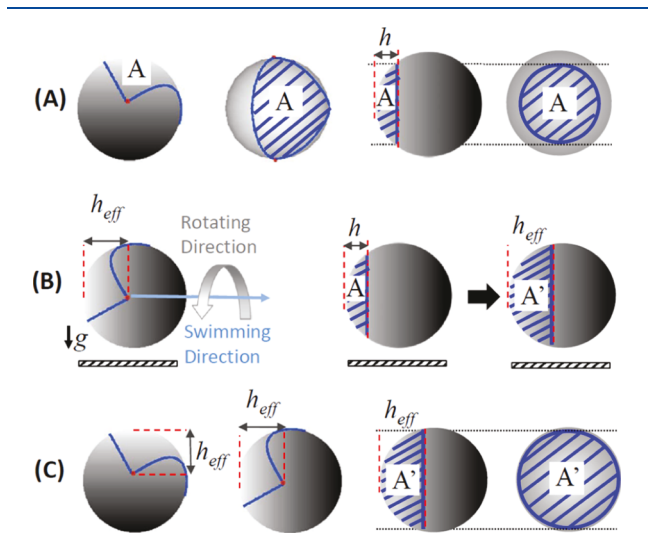


Figure 5. Illustration of assumptions made for phoretic velocity calculations. (A) Symmetric cap of height h and area A (from left to right: side and top view of actual catalytic patch area A on the patchy swimmer and side and top view of the symmetric patch of identical area A located at the pole of the particle). (B) Illustration of the interaction between the patchy swimmer and nearby wall indicating the swimming direction, rotation around the swimming axis, gravitational force g, and resulting increase of patch height from h to $h_{\rm eff}$ (see text). (C) Pseudo-hemispherical cap of height $h_{\rm eff}$ and area A' [from left to right: side and top view of actual catalytic patch area A on the patchy swimmer and side and top view of pseudo-hemispherical patch with larger area A' located at the pole of the particle caused by rotation around the swimming axis as shown in (B)].

velocities and confirming the accuracy of the parameters used in our velocity prediction. It is worth noting that the phoretic velocities for the 2.4 and 5 μ m particles show only a weak dependence on particle size in good agreement with the literature prediction.³¹

A rationale for the observed discrepancy might be found in the assumptions made regarding the patch shape and position for the analytically calculated velocities. Figure 5 illustrates the various assumptions made in the phoretic velocity calculations. As noted earlier and illustrated in Figure 5A, the analytical expression used for the phoretic velocities represented by the dashed line is derived based on the assumption that patchy swimmers have a hemispherical patch with an area A identical to that of the patchy particle located symmetrically at the pole of the particle (Figure 5A, right), whereas the actual patch area of the patchy swimmers is asymmetric as shown in Figure 1 and illustrated in the left half of Figure 5A.

A possible approach to account for the effect of patch asymmetry in the model in order to correctly predict the phoretic velocities is presented in Figure 5B. For the case of an asymmetric patch, a new parameter—the effective height of the patch (h_{eff}) —is defined, based on the assumption that the particle is moving in the direction of the maximum oxygen concentration, i.e., the swimming direction. The swimming direction is defined perpendicular to the longest line within the patch surface and parallel to h_{eff} (Figure 5B, left and Table S2). As it moves, the patchy swimmer rotates around its swimming axis with respect to the patch leading to a pseudo-hemispherical patch with a larger surface area A'. Figure 5C illustrates in more detail the transformation from an asymmetric patch with surface area, A, to a pseudo-hemispherical patch with increased surface area, A'. The larger area A' then supports the higher experimental velocities observed for the patchy swimmers.

Next, we provide a discussion on why a preferential rotation around the swimming direction is possible in the patchy particle system. According to the phoretic mechanism, which drives the motion of the particle, the catalytic chemical reaction on the active side of the particle releases solute in the surrounding of the particles. The closeness of the bottom cell wall may distort the solute gradient and fluid distribution around the particle.^{39,40} As a result, the hydrodynamic interactions between the wall and the particle contribute to the orientation of the swimming particle near the wall such that it preferentially rotates around its swimming axis as illustrated in the left half of Figure 5B. This preferential orientation has been experimentally confirmed in the case of Janus swimmers by Ebbens and Howse³⁶ and has also been observed in biological systems.⁵⁵ Utilizing the effective height parameter allows the calculation of a pseudo-hemispherical patch (see Table S2) with a larger area A' resulting in revised S_b values for the 11- and 25%-coated patchy swimmers, which result in the phoretic velocities plotted in Figure 4 (black solid line/black triangles). The error bars on the calculated phoretic velocities in Figure 4 are an indication of the effect of the broad range of patch geometries accessible for the smaller patch sizes caused by variations in the monolayer orientation.⁴⁶ For a particular patch size, S_h is calculated for the various patch shapes accessible and the error bar indicates the range of phoretic velocities expected considering the smallest and largest h_{eff} (see Table S2). As shown in Figure 4, the phoretic velocities calculated using the $h_{\rm eff}$ parameter, that is, the pseudo-hemispherical cap, show excellent agreement with the experimental velocities confirming the applicability of the selfdiffusiophoresis mechanism and the preferential alignment of patchy swimmers due to the particle-wall interactions. Additionally, as the patch size becomes larger, patches become more and more symmetric diminishing the effect of the patch

shape (smaller error bars). Interestingly, we do not observe spiral trajectories as reported by Ebbens et al.⁴⁵ Potential reasons for the observed differences in patchy swimmer trajectories are differences in Pt cap thickness or roughness used in the two studies.

CONCLUSIONS

We have studied the motion of a class of active colloids by experimentally tuning the surface activity of particles. Our ability to design patchy swimmers with well-defined swimming properties using the glancing angle deposition method yielded controlled patch geometries. The particle motion of the patchy swimmers is attributed to the self-generated concentration gradient of O2 created by the catalytic activity of Pt patches covering between 0 and 50% of the particle surface. Our study demonstrates that as the patch size increases, the particle velocity increases accordingly as well as the particles exhibit enhanced motion, addressing the far-reaching potential application of active colloids. We show that it is possible to control the active motion of the particles by controlling the surface properties rather than changing the environment of the active colloid. Furthermore, our investigation highlights the effect of the wall on the motion of the patchy swimmers leading to the preferential orientation and rotational motion because of the hydrodynamic interaction between the particle and the solid boundary, which verifies predictions from previous theoretical studies. 15,17,34 Further, our experimental study sheds light on the behavior of patchy swimmers, evoking the necessity of more insight into the self-induced phoretic motion to better understand the principles underlying the phoretic mechanism.

ASSOCIATED CONTENT

S Supporting Information

The Supporting Information is available free of charge on the ACS Publications website at DOI: 10.1021/acs.langmuir.8b03220.

Particle trajectory analysis, effect of the monolayer orientation on $h_{\rm eff}$ calculation, and motion of patchy swimmers (PDF)

Motion of 2.4 μ m particles with 0% patch in 3% (v/v) aqueous H₂O₂ solution (AVI)

Motion of 2.4 μ m particles with 11% patch in 3% (v/v) aqueous H_2O_2 solution (AVI)

Motion of 2.4 μ m particles with 25% patch in 3% (v/v) aqueous H₂O₂ solution (AVI)

Motion of 2.4 μ m particles with 50% patch in 3% (v/v) aqueous H₂O₂ solution (AVI)

Motion of 5 μ m particles with 11% patch in 3% (v/v) aqueous H₂O₂ solution (AVI)

Motion of 5 μ m particles with 25% patch in 3% (v/v) aqueous H₂O₂ solution (AVI)

Motion of 5 μ m particles with 50% patch in 3% (v/v) aqueous H_2O_2 solution (AVI)

Motion of 5 μ m particles with 50% patch in aqueous solution (AVI)

AUTHOR INFORMATION

Corresponding Author

*E-mail: kretzschmar@ccny.cuny.edu.

ORCID ®

Ilona Kretzschmar: 0000-0001-7636-1679

Present Address

[†]Momentive Performance Materials, 769 Old Saw Mill River Road, Tarrytown, NY 10591.

Author Contributions

The manuscript was written through contributions of all authors. All authors have given approval to the final version of the manuscript.

Notes

The authors declare no competing financial interest.

ACKNOWLEDGMENTS

This work was supported by the National Science Foundation under Award CBET-1264550. Z.J. acknowledges a fellowship from Mr. Leonard Schuchman.

REFERENCES

- (1) Patra, D.; Sengupta, S.; Duan, W.; Zhang, H.; Pavlick, R.; Sen, A. Intelligent, self-powered, drug delivery systems. *Nanoscale* **2013**, *5*, 1273–1283.
- (2) JianFeng; Cho, S. Mini and Micro Propulsion for Medical Swimmers. *Micromachines* **2014**, *5*, 97–113.
- (3) Sundararajan, S.; Lammert, P. E.; Zudans, A. W.; Crespi, V. H.; Sen, A. Catalytic Motors for Transport of Colloidal Cargo. *Nano Lett.* **2008**, *8*, 1271–1276.
- (4) Ghalanbor, Z.; Marashi, S.-A.; Ranjbar, B. Nanotechnology helps medicine: Nanoscale swimmers and their future applications. *Med. Hypotheses* **2005**, *65*, 198–199.
- (5) Wang, J.; Gao, W. Nano/Microscale Motors: Biomedical Opportunities and Challenges. ACS Nano 2012, 6, 5745–5751.
- (6) Baraban, L.; Makarov, D.; Streubel, R.; Mönch, I.; Grimm, D.; Sanchez, S.; Schmidt, O. G. Catalytic Janus Motors on Microfluidic Chip: Deterministic Motion for Targeted Cargo Delivery. *ACS Nano* **2012**, *6*, 3383–3389.
- (7) Balasubramanian, S.; Kagan, D.; Jack Hu, C.-M.; Campuzano, S.; Lobo-Castañon, M. J.; Lim, N.; Kang, D. Y.; Zimmerman, M.; Zhang, L.; Wang, J. Micromachine-Enabled Capture and Isolation of Cancer Cells in Complex Media. *Angew. Chem., Int. Ed.* **2011**, *50*, 4161–4164.
- (8) Li, J.; Shklyaev, O. E.; Li, T.; Liu, W.; Shum, H.; Rozen, I.; Balazs, A. C.; Wang, J. Self-Propelled Nanomotors Autonomously Seek and Repair Cracks. *Nano Lett.* **2015**, *15*, 7077–7085.
- (9) Loget, G.; Kuhn, A. Bulk synthesis of Janus objects and asymmetric patchy particles. J. Mater. Chem. 2012, 22, 15457–15474.
- (10) Pawar, A. B.; Kretzschmar, I. Fabrication, Assembly, and Application of Patchy Particles. *Macromol. Rapid Commun.* **2010**, *31*, 150–168.
- (11) Vaccari, L.; Molaei, M.; Leheny, R. L.; Stebe, K. J. Cargo carrying bacteria at interfaces. *Soft Matter* **2018**, *14*, 5643–5653.
- (12) Gao, W.; Wang, J. The Environmental Impact of Micro/Nanomachines: A Review. ACS Nano 2014, 8, 3170-3180.
- (13) Parmar, J.; Ma, X.; Katuri, J.; Simmchen, J.; Stanton, M. M.; Trichet-Paredes, C.; Soler, L.; Sanchez, S. Nano and micro architectures for self-propelled motors. *Sci. Technol. Adv. Mater.* **2015**, *16*, 014802.
- (14) Parmar, J.; Vilela, D.; Villa, K.; Wang, J.; Sánchez, S. Micro- and Nanomotors as Active Environmental Microcleaners and Sensors. *J. Am. Chem. Soc.* **2018**, *140*, 9317–9331.
- (15) Wang, S.; Wu, N. Selecting the Swimming Mechanisms of Colloidal Particles: Bubble Propulsion versus Self-Diffusiophoresis. *Langmuir* **2014**, *30*, 3477–3486.
- (16) Gao, W.; Sattayasamitsathit, S.; Orozco, J.; Wang, J. Highly Efficient Catalytic Microengines: Template Electrosynthesis of Polyaniline/Platinum Microtubes. *J. Am. Chem. Soc.* **2011**, *133*, 11862–11864.
- (17) Gregory, D. A.; Campbell, A. I.; Ebbens, S. J. Effect of Catalyst Distribution on Spherical Bubble Swimmer Trajectories. *J. Phys. Chem. C* **2015**, *119*, 15339–15348.

(18) Solovev, A. A.; Mei, Y.; Bermúdez Ureña, E.; Huang, G.; Schmidt, O. G. Catalytic Microtubular Jet Engines Self-Propelled by Accumulated Gas Bubbles. *Small* **2009**, *5*, 1688–1692.

- (19) Gao, W.; Sattayasamitsathit, S.; Wang, J. Catalytically propelled micro-/nanomotors: how fast can they move? *Chem. Rec.* **2012**, *12*, 224–231
- (20) Nourhani, A.; Crespi, V. H.; Lammert, P. E.; Borhan, A. Self-electrophoresis of spheroidal electrocatalytic swimmers. *Phys. Fluids* **2015**, 27, 092002.
- (21) Ebbens, S.; Gregory, D. A.; Dunderdale, G.; Howse, J. R.; Ibrahim, Y.; Liverpool, T. B.; Golestanian, R. Electrokinetic effects in catalytic platinum-insulator Janus swimmers. *Europhys. Lett.* **2014**, *106*, 58003.
- (22) Wang, Y.; Hernandez, R. M.; Bartlett, D. J.; Bingham, J. M.; Kline, T. R.; Sen, A.; Mallouk, T. E. Bipolar Electrochemical Mechanism for the Propulsion of Catalytic Nanomotors in Hydrogen Peroxide Solutions. *Langmuir* **2006**, 22, 10451–10456.
- (23) Paxton, W. F.; Baker, P. T.; Kline, T. R.; Wang, Y.; Mallouk, T. E.; Sen, A. Catalytically Induced Electrokinetics for Motors and Micropumps. *J. Am. Chem. Soc.* **2006**, *128*, 14881–14888.
- (24) Mano, N.; Heller, A. Bioelectrochemical Propulsion. *J. Am. Chem. Soc.* **2005**, *127*, 11574–11575.
- (25) Paxton, W. F.; Sen, A.; Mallouk, T. E. Motility of Catalytic Nanoparticles through Self-Generated Forces. *Chem.—Eur. J.* **2005**, *11*. 6462–6470.
- (26) Golestanian, R.; Liverpool, T. B.; Ajdari, A. Propulsion of a Molecular Machine by Asymmetric Distribution of Reaction Products. *Phys. Rev. Lett.* **2005**, *94*, 220801.
- (27) Golestanian, R.; Liverpool, T. B.; Ajdari, A. Designing phoretic micro- and nano-swimmers. *New J. Phys.* **2007**, *9*, 126.
- (28) Howse, J. R.; Jones, R. A. L.; Ryan, A. J.; Gough, T.; Vafabakhsh, R.; Golestanian, R. Self-Motile Colloidal Particles: From Directed Propulsion to Random Walk. *Phys. Rev. Lett.* **2007**, 99, 048102.
- (29) Popescu, M. N.; Dietrich, S.; Tasinkevych, M.; Ralston, J. Phoretic motion of spheroidal particles due to self-generated solute gradients. *Eur. Phys. J. E: Soft Matter Biol. Phys.* **2010**, 31, 351–367.
- (30) Vicario, J.; Eelkema, R.; Browne, W. R.; Meetsma, A.; La Crois, R. M.; Feringa, B. L. Catalytic molecular motors: fuelling autonomous movement by a surface bound synthetic manganese catalase. *Chem. Commun.* **2005**, 3936–3938.
- (31) Ebbens, S.; Tu, M.-H.; Howse, J. R.; Golestanian, R. Size dependence of the propulsion velocity for catalytic Janus-sphere swimmers. *Phys. Rev. E: Stat., Nonlinear, Soft Matter Phys.* **2012**, 85, No. 020401(R).
- (32) Dunderdale, G.; Ebbens, S. Directed Propulsion, Chemotaxis and Clustering in Propelled Microparticles. *Curr. Phys. Chem.* **2015**, *5*, 91–106.
- (33) Zheng, X.; Wu, M.; Kong, F.; Cui, H.; Silber-Li, Z. Visualization and measurement of the self-propelled and rotational motion of the Janus microparticles. *J. Visualization* **2015**, *18*, 425–435.
- (34) Brown, A. T.; Poon, W. C. K.; Holm, C.; de Graaf, J. Ionic screening and dissociation are crucial for understanding chemical self-propulsion in polar solvents. *Soft Matter* **2017**, *13*, 1200–1222.
- (35) Brown, A.; Poon, W. Ionic effects in self-propelled Pt-coated Janus swimmers. *Soft Matter* **2014**, *10*, 4016–4027.
- (36) Ebbens, S. J.; Howse, J. R. Direct Observation of the Direction of Motion for Spherical Catalytic Swimmers. *Langmuir* **2011**, 27, 12293–12296.
- (37) Das, S.; Garg, A.; Campbell, A. I.; Howse, J.; Sen, A.; Velegol, D.; Golestanian, R.; Ebbens, S. J. Boundaries can steer active Janus spheres. *Nat. Commun.* **2015**, *6*, 8999.
- (38) Crowdy, D. G. Wall effects on self-diffusiophoretic Janus particles: a theoretical study. *J. Fluid Mech.* **2013**, *735*, 473–498.
- (39) Ibrahim, Y.; Liverpool, T. B. The dynamics of a self-phoretic Janus swimmer near a wall. *Europhys. Lett.* **2015**, *111*, 48008.
- (40) Uspal, W. E.; Popescu, M. N.; Dietrich, S.; Tasinkevych, M. Self-propulsion of a catalytically active particle near a planar wall:

from reflection to sliding and hovering. Soft Matter 2015, 11, 434-438.

- (41) Simmchen, J.; Katuri, J.; Uspal, W. E.; Popescu, M. N.; Tasinkevych, M.; Sánchez, S. Topographical pathways guide chemical microswimmers. *Nat. Commun.* **2016**, *7*, 10598.
- (42) Das, S.; Shklyaev, O. E.; Altemose, A.; Shum, H.; Ortiz-Rivera, I.; Valdez, L.; Mallouk, T. E.; Balazs, A. C.; Sen, A. Harnessing catalytic pumps for directional delivery of microparticles in microchambers. *Nat. Commun.* **2017**, *8*, 14384.
- (43) Katuri, J.; Caballero, D.; Voituriez, R.; Samitier, J.; Sanchez, S. Directed Flow of Micromotors through Alignment Interactions with Micropatterned Ratchets. *ACS Nano* **2018**, *12*, 7282–7291.
- (44) Graaf, J. d.; Rempfer, G.; Holm, C. Diffusiophoretic Self-Propulsion for Partially Catalytic Spherical Colloids. *IEEE Trans. NanoBioscience* **2015**, *14*, 272–288.
- (45) Archer, R. J.; Campbell, A. I.; Ebbens, S. J. Glancing angle metal evaporation synthesis of catalytic swimming Janus colloids with well defined angular velocity. *Soft Matter* **2015**, *11*, 6872–6880.
- (46) Pawar, A. B.; Kretzschmar, I. Patchy Particles by Glancing Angle Deposition. *Langmuir* **2008**, 24, 355–358.
- (47) Pawar, A. B.; Kretzschmar, I. Multifunctional Patchy Particles by Glancing Angle Deposition. *Langmuir* **2009**, *25*, 9057–9063.
- (48) Crocker, J. C.; Hoffman, B. D. Multiple-Particle Tracking and Two-Point Microrheology in Cells. *Methods in Cell Biology*; Academic Press, 2007; Vol. 83, pp 141–178.
- (49) Dunderdale, G.; Ebbens, S.; Fairclough, P.; Howse, J. Importance of Particle Tracking and Calculating the Mean-Squared Displacement in Distinguishing Nanopropulsion from Other Processes. *Langmuir* **2012**, *28*, 10997–11006.
- (50) Crocker, J. C. Measurement of the hydrodynamic corrections to the Brownian motion of two colloidal spheres. *J. Chem. Phys.* **1997**, *106*, 2837–2840.
- (51) Paxton, W. F.; Kistler, K. C.; Olmeda, C. C.; Sen, A.; St. Angelo, S. K.; Cao, Y.; Mallouk, T. E.; Lammert, P. E.; Crespi, V. H. Catalytic Nanomotors: Autonomous Movement of Striped Nanorods. *J. Am. Chem. Soc.* **2004**, *126*, 13424–13431.
- (52) Paxton, W. F.; Sundararajan, S.; Mallouk, T. E.; Sen, A. Chemical Locomotion. *Angew. Chem., Int. Ed.* **2006**, 45, 5420–5429.
- (53) Córdova-Figueroa, U. M.; Brady, J. F. Osmotic Propulsion: The Osmotic Motor. *Phys. Rev. Lett.* **2008**, *100*, 158303.
- (54) Anderson, J. L. Colloid Transport by Interfacial Forces. *Annu. Rev. Fluid Mech.* **1989**, 21, 61–99.
- (55) Berke, A. P.; Turner, L.; Berg, H. C.; Lauga, E. Hydrodynamic Attraction of Swimming Microorganisms by Surfaces. *Phys. Rev. Lett.* **2008**, *101*, 038102.